Cancer Cell
Article

Targeted Inactivation of Mdm2 RING Finger E3 Ubiquitin Ligase Activity in the Mouse Reveals Mechanistic Insights into p53 Regulation

Koji Itahana,[1,2] Hua Mao,[1,2] Aiwen Jin,[1] Yoko Itahana,[1,2] Hilary V. Clegg,[2,4] Mikael S. Lindström,[1,2] Krishna P. Bhat,[6] Virginia L. Godfrey,[5] Gerard I. Evan,[7] and Yanping Zhang[1,2,3,*]
[1]Department of Radiation Oncology
[2]Lineberger Comprehensive Cancer Center
[3]Department of Pharmacology
[4]Curriculum in Genetics and Molecular Biology
[5]Department of Pathology
School of Medicine, the University of North Carolina at Chapel Hill, Chapel Hill, NC 27599-7512, USA
[6]Department of Pathology, Section of Neuropathology, University of Texas M.D. Anderson Cancer Center, Houston, TX 77030, USA
[7]Cancer Research Institute and Department of Cellular and Molecular Pharmacology, Comprehensive Cancer Center, University of California, San Francisco, San Francisco, CA 94143, USA
*Correspondence: ypzhang@med.unc.edu
DOI 10.1016/j.ccr.2007.09.007

SUMMARY

It is believed that Mdm2 suppresses p53 in two ways: transcriptional inhibition by direct binding, and degradation via its E3 ligase activity. To study these functions physiologically, we generated mice bearing a single-residue substitution (C462A) abolishing the E3 function without affecting p53 binding. Unexpectedly, homozygous mutant mice died before E7.5, and deletion of p53 rescued the lethality. Furthermore, reintroducing a switchable p53 by crossing with *p53ER^{TAM}* mice surprisingly demonstrated that the mutant Mdm2^{C462A} was rapidly degraded in a manner indistinguishable from that of the wild-type Mdm2. Hence, our data indicate that (1) the Mdm2-p53 physical interaction, without Mdm2-mediated p53 ubiquitination, cannot control p53 activity sufficiently to allow early mouse embryonic development, and (2) Mdm2's E3 function is not required for Mdm2 degradation.

INTRODUCTION

The transcription factor p53 responds to DNA damage and other cellular stressors by inducing cell cycle arrest or apoptosis, thereby playing a critical role in tumor suppression. It is well established that Mdm2 is the major negative regulator of the tumor suppressor p53, yet the mechanism by which Mdm2 suppresses p53 remains inadequately understood. The prevailing view of Mdm2-mediated p53 inhibition is that Mdm2 suppresses p53 via a "dual" mechanism—Mdm2 binds to and masks p53's N-terminal transactivation domain, directly interfering with p53's ability to recruit basal transcriptional machinery (Momand et al., 1992; Oliner et al., 1993; Thut et al., 1997), and/or promotes ubiquitin-mediated degradation of p53 (Haupt et al., 1997; Honda et al., 1997; Kubbutat et al., 1997).

Studies supporting the masking mechanism include findings that mutations in the transactivation domain of p53 that impair its binding with components of the transcription machinery also disrupt its binding with Mdm2 (Lin et al., 1994), suggesting that Mdm2 and the basal transcription factors competitively interact with overlapping sequences in p53 (reviewed in Ko and Prives, 1996). In addition, when recruited to a promoter by fusion

SIGNIFICANCE

Mdm2 is frequently amplified or overexpressed in human cancers, many of which lack mutations in the *p53* tumor suppressor gene; thus, it is believed that Mdm2 overexpression is functionally equivalent to p53 mutation. Current dogma holds that Mdm2 binding alone is sufficient to block p53's transcriptional activity. In contrast, our in vivo data show that Mdm2 binding does not adequately repress p53, at least not to an extent allowing mouse embryo development. Furthermore, we show that Mdm2 autodegradation is not the principle mechanism for Mdm2 degradation in vivo. Our in vivo evidence calls for a revision to current dogma regarding Mdm2's regulation of both p53 and itself.

with a heterologous Gal4 DNA-binding domain, Mdm2 is capable of repressing basal transcription via a sequence, comprising Mdm2 residues 50–222, that appears to be separate from its p53-binding site (Thut et al., 1997). Notably, this inhibitory domain overlaps with an Mdm2 domain at residues 102–222 that is required for binding with the transcription cofactor p300/CBP (Grossman et al., 1998), suggesting that Mdm2 could interfere with p53 transcription through interaction with these cofactors, given that p300/CBP augments p53 transcriptional activity by promoting acetylation of p53 C-terminal lysine residues. Intriguingly, these C-terminal acetylation sites of p53 are also essential for Mdm2-induced ubiquitination and subsequent degradation of p53, thus indicating a potential connection between p53 transcriptional function and Mdm2-induced ubiquitination. However, it has not been shown whether Mdm2-p53 binding alone is sufficient, or whether Mdm2-mediated ubiquitination is also required, for Mdm2 to repress p53.

Mdm2-mediated p53 ubiquitination and degradation have drawn significant attention in recent years. Mdm2 belongs to a large family of RING finger ubiquitin ligases. The RING finger motif is characterized by a group of conserved cysteine and histidine residues that form a cross-brace structure upon binding of two zinc ions. This structure interacts with E2 ubiquitin-conjugating enzymes and facilitates ubiquitination of bound substrates. Mdm2's ligase activity is completely abolished by mutations at any of the eight cysteine and histidine residues involved in zinc coordination, and it can also be inhibited by a metal chelator, indicating a requirement for the correct zinc-dependent folding of the RING finger. It is now generally accepted that Mdm2 is the principal p53 ubiquitin ligase (Yang et al., 2004). Mice with targeted deletion of the *Mdm2* gene die during early embryonic development, and this lethality can be rescued by concomitant deletion of *p53*, indicating that the embryonic lethality of *Mdm2* null mice is due to activation of p53 (Jones et al., 1995; Luna et al., 1995).

Functions other than E3 ubiquitin ligase activity have been ascribed to the Mdm2 RING domain. For example, this region of Mdm2 can bind to RNA (Elenbaas et al., 1996), and it also harbors a cryptic nucleolar localization signal that is exposed under certain circumstances such as p14ARF binding (Lohrum et al., 2000). Moreover, the Mdm2 RING domain can bind nucleotides such as ATP, an activity important for Mdm2 nucleolar localization (Poyurovsky et al., 2003). Recently, it was shown that the RING domain of Mdm2 forms a spontaneously assembled supramolecular complex in solution (Poyurovsky et al., 2007). The Mdm2 RING domain also mediates homodimerization with itself and heterodimerization with MDMX (Jackson and Berberich, 2000; Sharp et al., 1999; Stad et al., 2000; Tanimura et al., 1999), findings confirmed recently in a paper describing the NMR solution structure of the Mdm2 RING domain dimer (Kostic et al., 2006).

In this study, we generated and investigated mice bearing a single-residue substitution, C462A, in the RING finger domain of Mdm2. Our mouse model reveals two unexpected insights into the mechanism for Mdm2 RING-mediated E3 ligase activity: (1) the Mdm2-p53 physical interaction alone, without Mdm2-mediated p53 ubiquitination, is unable to suppress p53 activity; and (2) the Mdm2 RING-mediated E3 ubiquitin ligase function is dispensable for Mdm2 degradation.

RESULTS

Mice Homozygous for *Mdm2 C462A* Mutation Die during Embryonic Development

To investigate the in vivo function of the Mdm2 RING finger E3 ubiquitin ligase, we engineered a Cys-to-Ala substitution at the zinc-coordinating residue C462 in the mouse Mdm2 (equivalent to C464 in human HDM2) (Figure 1A). This mutation, which alters a structural-crucial zinc coordinating cysteine, has been shown to abolish Mdm2's E3 ubiquitin ligase activity without affecting Mdm2-p53 binding (Geyer et al., 2000). Correct targeting of the *Mdm2* allele by a substitution of TGT > GCC in codon 462, which simultaneously generates an *Eag1* restriction site (CGGCCG), was confirmed by Southern blotting (Figure 1B) and by *Eag1* digestion of PCR-amplified genomic DNA (Figure 1C) from the targeted embryonic stem (ES) cells. The targeted allele was reconfirmed by sequencing of the mouse genomic DNA after germline transmission was obtained (Figure 1D). The *neomycin resistance* gene was subsequently removed from the targeted allele by crossing the $Mdm2^{+/C462A}$ heterozygous mice with transgenic mice expressing *Cre* recombinase.

Mice heterozygous for the $Mdm2^{C462A}$ allele ($Mdm2^{+/C462A}$) appeared phenotypically normal and fertile. The $Mdm2^{+/C462A}$ mice were intercrossed, and the offspring were genotyped by PCR of genomic DNA isolated from tail biopsies. Of the 127 progeny obtained from the intercrosses, 41 (32%) were wild-type for *Mdm2* ($Mdm2^{+/+}$), and 86 (68%) were heterozygous for the targeted *Mdm2* allele, in agreement with the expected 1:2 ratio from the cross. No viable $Mdm2^{C462A}$ homozygous mutant mice were detected (Table 1), indicating that homozygosity for the targeted *Mdm2* allele ($Mdm2^{C462A/C462A}$) leads to embryonic lethality.

To determine the gestational time of the embryonic lethality for the $Mdm2^{C462A/C462A}$ mice, genomic DNA was isolated from the yolk sacs of embryos harvested at various gestational stages from intercrosses of $Mdm2^{+/C462A}$ mice and analyzed by PCR to detect the presence of $Mdm2^{C462A/C462A}$ embryos. Of the 81 embryos isolated from embryonic day (E) 8.5 to 13.5, 19 (23%) were $Mdm2^{+/+}$, 41 (51%) were $Mdm2^{+/C462A}$, and 21 (26%) were empty deciduae or embryos at various stages of reabsorption (Table 2). These three types of embryos fall into a ratio of approximately 1:2:1, as expected for a heterozygous intercross. We were unable to isolate DNA, without contamination from outside tissues, from the partially reabsorbed embryos. We believe that these reabsorbed embryos are $Mdm2^{C462A/C462A}$ homozygous. Thus, the

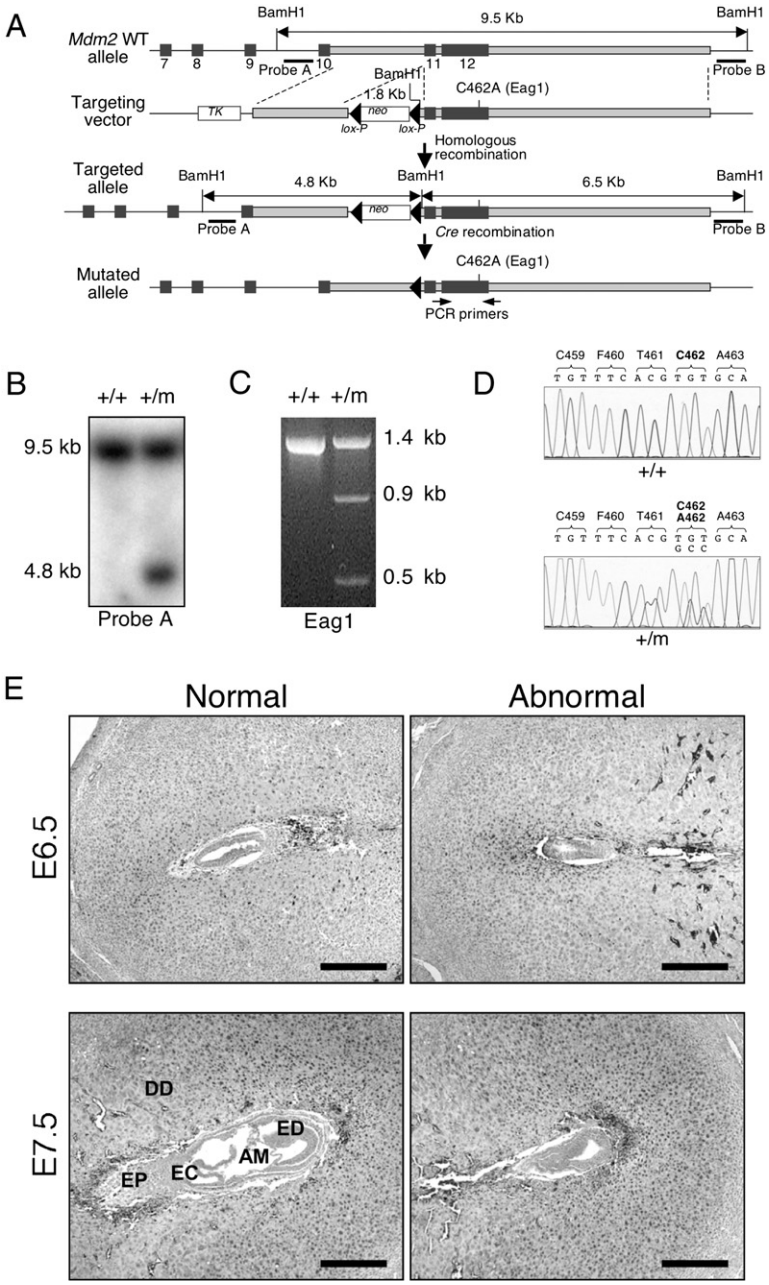

Figure 1. Generation of *Mdm2*^{C462A} Knockin Mice

(A) Schematic representation of the *Mdm2* gene-targeting vector. The black boxes represent the last six exons of the *Mdm2* gene, with exon numbers indicated. The gray boxes of intermediate thickness represent vector homology to the target locus in the chromosome. The open boxes are the selection markers. The triangles indicate *loxP* sites with orientations pointed. Southern blot analysis was used to screen the targeted allele. BamH1 digestion generates a 9.5 Kb fragment from the wild-type allele that can be detected by probes A and B. The targeted allele gives rise to two BamH1 fragments of 4.8 Kb and 6.5 Kb, which can be detected by probes A or B, respectively. The clones containing the C > A mutation on codon 462 were screened by PCR using primers shown by arrows below exon 12 and by digestion of the Eag1 site that was introduced with the mutation. (Diagram is not to scale.)

(B) Correctly targeted ES cells were identified by Southern blotting using BamH1-digested DNA and a 1 Kb DNA fragment as probe (probe A). +/+, wild-type *Mdm2* locus; +/m, *Mdm2*$^{+/C462A}$ heterozygous locus.

(C) PCR amplification of genomic DNA from *Mdm2*$^{+/m}$ cells using a primer set (indicated in [A]) and confirmation of the presence of the C462A mutation by Eag1 digestion are shown.

(D) Sequencing results of wild-type and mutant alleles of Mdm2. Genomic DNA was isolated from tail biopsies of three-week-old mice, amplified by PCR using primers shown in (A), and then sequenced. Note that the Cys > Ala mutation at codon 462 results in an Eag1 restriction site (CGGCCG).

(E) Histological analysis of embryos harvested from *Mdm2*$^{+/m}$ intercrosses on day 6.5 (E6.5) and 7.5 (E7.5) of gestation. Littermate normal and abnormal embryos are shown. AM, amnion; DD, decidua; EC, ectoplacental cavity; ED, ectoderm; EP, ectoplacental cone. Scale bar, 400 μm.

Mdm2$^{C462A/C462A}$ embryos must have died prior to E8.5 of gestation.

To establish a more specific timeline for the embryonic lethality, histological analysis of embryos at E6.5–E9.5 was performed. All embryos examined at E6.5 of gestation exhibited visible embryonic architecture (Figure 1E), although approximately one-fourth of the embryos appeared somewhat smaller than the others (indicated as "abnormal"). At E7.5, most embryos exhibited features characteristic of normal development, including gastrulation, initiation of organogenesis, differentiation of the three germ layers (ectoderm, mesoderm, and endoderm), and formation of the three embryonic cavities (ectoplacental, exocoel, and amniotic). In contrast, of the 24 total dissected E7.5 deciduae, 5 (21%) were found to be smaller in size than normal E7.5 embryos and exhibited none of the developmental features of normal E7.5 embryos (Figure 1E); instead, the smaller embryos exhibited a size and structure similar to that of E6.5 embryos (e.g., differentiation of proamniotic cavity and extraembryonic ectoderm). Beyond E7.5, only empty cavities, but not embryos, were evident from the smaller deciduae, most likely resulting from reabsorption of abnormal embryos (data not shown). Of the 93 deciduae examined from 11 female mice at E6.5, E7.5, and E8.5, 27 (29%) exhibited either abnormal or empty embryonic architecture. The abnormal

Table 1. Genotypes of Mice Resulting from *Mdm2*$^{+/C462A}$ Intercrosses

Total No. of Mice	+/+	+/*m*	*m*/*m*
127	41 (32%)	86 (68%)	0

PCR-based genotyping was performed with genomic DNA isolated from tail biopsies. +/+, wild type *Mdm2*; +/m, *Mdm2*$^{+/C462A}$; m/m, *Mdm2*$^{C462A/C462A}$.

embryos varied in architecture, but all were smaller than the normal littermates and failed to undergo proper gastrulation. Hence, these results suggest that the *Mdm2*$^{C462A/C462A}$ homozygous mutation produces developmental retardation and causes embryonic lethality prior to E7.5 of gestation. Of note, the embryonic lethality resulting from *Mdm2* knockout (*Mdm2*$^{-/-}$) happens immediately after implantation, which occurs at E5.5 (Jones et al., 1995; Luna et al., 1995). Thus, the *Mdm2*$^{C462A/C462A}$ embryos die at a developmental stage slightly later than, but approximately comparable to, that of *Mdm2*$^{-/-}$ embryos.

Mdm2^{C462A} Homozygous Embryonic Lethality Can Be Rescued by Concomitant Deletion of p53

It has been shown previously that the embryonic lethality of *Mdm2*$^{-/-}$ mice can be rescued by concomitant deletion of *p53*, indicating that the lethality in *Mdm2* null mice results from unchecked p53 function (Jones et al., 1995; Luna et al., 1995). We therefore investigated whether the embryonic lethality of *Mdm2*$^{C462A/C462A}$ mice was also due to the inability of the mutant Mdm2 to suppress p53. The *Mdm2*$^{+/C462A}$ heterozygous mice were crossed with *p53* null (*p53*$^{-/-}$) mice to generate *Mdm2*$^{+/C462A}$;*p53*$^{+/-}$ mice, which were then intercrossed to generate *Mdm2*$^{C462A/C462A}$;*p53*$^{-/-}$ double-homozygous mice. We successfully recovered *Mdm2*$^{C462A/C462A}$;*p53*$^{-/-}$ mice at the expected Mendelian ratio (Figure 2A), and the double-homozygous mice appeared morphologically indistinguishable from other littermates (data not shown). Correct targeting of the C462A codon was reconfirmed by sequencing of PCR-amplified genomic DNA isolated from the *Mdm2*$^{C462A/C462A}$;*p53*$^{-/-}$ mouse tail biopsies (Figure 2B). No homozygous *Mdm2*$^{C462A/C462A}$ mice were

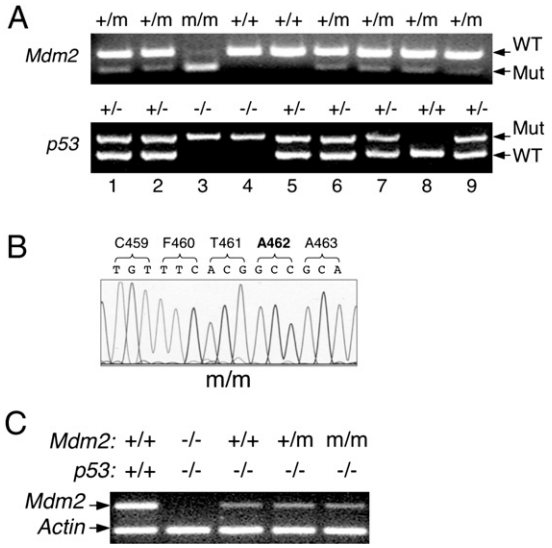

Figure 2. Crossing with *p53* Null Mice Rescues *Mdm2*$^{m/m}$ Homozygous Embryonic Lethality

(A) Genotyping of mice born from *Mdm2*$^{+/m}$;*p53*$^{+/-}$ mouse intercrosses. Genomic DNA was isolated from tail biopsies of three-week-old mice. For Mdm2 genotyping, DNA was PCR amplified with primers shown in Figure 1A and digested with Eag1. For p53 genotyping, the DNA was amplified using primers specific for mutant and wild-type alleles (information from The Jackson Laboratory). m/m, *Mdm2*$^{C462A/C462A}$ homozygous locus.

(B) DNA sequencing of PCR amplified tail biopsy DNA from *Mdm2*$^{m/m}$;*p53*$^{-/-}$ homozygous mice.

(C) Analysis of *Mdm2* gene expression. Total RNA was isolated from passage 1 MEFs and analyzed by RT-PCR (upper panel). *Actin* was coamplified as a loading control.

obtained with a heterozygous *p53* background (*Mdm2*$^{C462A/C462A}$;*p53*$^{+/-}$), indicating that heterozygosity of *p53* is not sufficient to rescue the embryonic lethality of *Mdm2*$^{C462A/C462A}$ mice. To demonstrate that the C462A mutation does not have aberrant consequences on *Mdm2* gene expression, we isolated mouse embryonic fibroblasts (MEFs) from littermate embryos and compared the expression of *Mdm2* mRNA by semiquantitative RT-PCR. *Mdm2* mRNA was expressed at equivalent levels in each of the three *p53* null MEFs, which expressed

Table 2. Genotypes of Embryos Resulting from *Mdm2*$^{+/C462A}$ Intercrosses

		Genotyped		
Gestational Age	Total No. of Embryos	+/+	+/*C462A*	No. of Reabsorptions
E13.5	13	3	7	3
E12.5	5	2	2	1
E11.5	7	2	4	1
E10.5	16	3	9	4
E9.5	17	4	8	5
E8.5	23	5	11	7
Total	81	19	41	21

PCR-based genotyping was performed with genomic DNA isolated from embryos at the indicated gestational days.

less *Mdm2* than the wild-type MEFs (Figure 2C), due to a lack of the Mdm2-transactivator p53. Thus, the $Mdm2^{C462A/C462A}$ homozygous embryonic lethality can be rescued by concomitant deletion of p53. These results indicate that the Mdm2 RING E3 ubiquitin ligase function is critically important for Mdm2 suppression of p53 in vivo, at least during early embryonic development.

Endogenous $Mdm2^{C462A}$ Is Fully Capable of Interacting with p53 but Not Sufficient to Suppress p53 Function

The embryonic lethality caused by the $Mdm2^{C462A}$ homozygous mutation, along with the rescue of the lethality by deletion of *p53*, indicates that the mutant Mdm2, although most likely capable of interacting with p53, is unable to control p53 activity sufficiently to allow early embryonic development. Previous in vitro studies have shown that the C462A mutation does not affect the Mdm2-p53 interaction (Honda and Yasuda, 2000). The early embryonic lethality of the mutant mice, however, barred us from addressing this issue directly in our mouse model. To solve this problem, we took advantage of a newly developed knockin mouse model in which the endogenous *p53* gene is replaced by one encoding $p53ER^{TAM}$ (p53ER thereafter), a fusion protein containing a full-length p53 fused C-terminally with the hormone-binding domain of a modified estrogen receptor. The p53 activity in the mice and MEFs can be rapidly switched between wild-type and knockout states by administration and withdrawal of 4-hydroxytamoxifen (4-OHT) (Christophorou et al., 2005). Because previous studies have shown that, under an *Mdm2* null background, two copies of the $p53ER^{TAM}$ allele ($p53^{ER/ER}$) could cause embryonic lethality (Ringshausen et al., 2006), we therefore bred $p53^{ER/-}$ mice into an $Mdm2^{C462A/C462A}$ background and isolated MEFs from $Mdm2^{C462A/C462A};p53^{ER/-}$ embryos. To determine the ability of p53ER to respond to 4-OHT in the $Mdm2^{C462A/C462A};p53^{ER/-}$ MEFs, we cultured early-passage cells (passage 2) in either the presence or absence of 4-OHT. We then assayed the expression of p53ER and two protein products of the p53 target genes, *Mdm2* and *p21*, at different time points after administration of 4-OHT. We used $Mdm2^{+/+};p53^{ER/-}$ MEFs (also passage 2) as controls. In the absence of 4-OHT (Figure 3A, lanes 1 and 6), $Mdm2^{C462A}$ protein was expressed at a low level, similar to that of wild-type Mdm2, and p21 expression was undetectable, consistent with the *p53* null status of the MEFs. On the other hand, the p53ER protein level was higher in the $Mdm2^{C462A/C462A};p53^{ER/-}$ MEFs than in the $Mdm2^{+/+};p53^{ER/-}$ MEFs, most likely due to lack of E3 activity of the $Mdm2^{C462A}$ protein. Upon 4-OHT treatment, the expression of Mdm2 was increased in both the $Mdm2^{C462A/C462A};p53^{ER/-}$ and the $Mdm2^{+/+};p53^{ER/-}$ MEFs, indicating the activation of p53ER, and this increase was considerably higher in the $Mdm2^{C462A/C462A};p53^{ER/-}$ MEFs than in the $Mdm2^{+/+};p53^{ER/-}$ MEFs (Figure 3A, Mdm2 panel). In the presence of 4-OHT, p53 was decreased in the $Mdm2^{+/+};p53^{ER/-}$ MEFs, due to expression of Mdm2, but was unchanged or slightly increased in the $Mdm2^{C462A/C462A};p53^{ER/-}$ MEFs (Figure 3A, p53 panel), indicating that the mutant $Mdm2^{C462A}$ cannot degrade p53. This is consistent with studies by other mouse models showing that Mdm2 is responsible for p53 degradation in vivo (Francoz et al., 2006; Toledo et al., 2006). Judging by a significantly high level of p21 activation in the $Mdm2^{C462A/C462A};p53^{ER/-}$ MEFs (Figure 3A, p21 panel), it is apparent that p53ER was activated even in the presence of high levels of the $Mdm2^{C462A}$ protein. This is consistent with our hypothesis that the $Mdm2^{C462A/C462A}$ mutant mouse embryos died

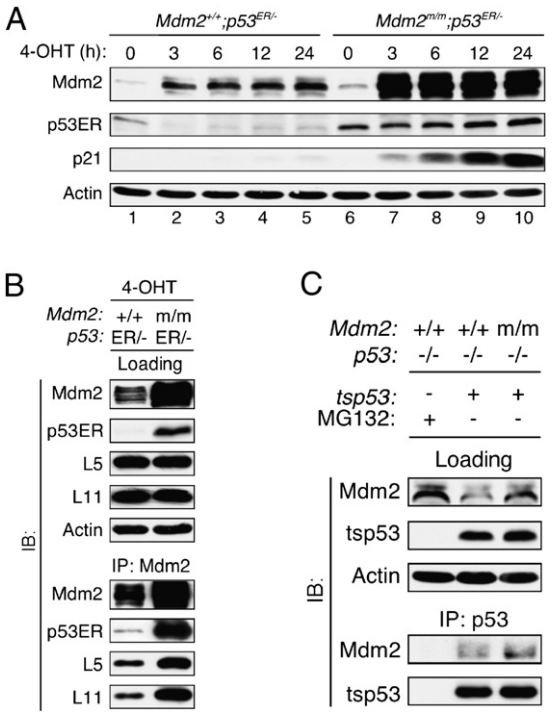

Figure 3. $Mdm2^{C462A}$ Mutant Protein Remains Fully Capable of Interacting with p53 but Is Unable to Suppress p53 Transcriptional Activity Sufficiently

(A) $Mdm2^{C462A}$ mutant is incapable of suppressing p53 transcriptional activity. Early-passage MEFs (passage 2) of $Mdm2^{+/+};p53^{ER/-}$ and $Mdm2^{m/m};p53^{ER/-}$ were prepared from embryos (E13.5) obtained by breeding $p53^{ER/-}$ mice into both $Mdm2^{+/+}$ and $Mdm2^{m/m}$ backgrounds. Cells were treated with ethanol (0 hr) or 100 nM of 4-hydroxytamoxifen (4-OHT) for the indicated lengths of time. The levels of Mdm2, p53ER, p21, and Actin were analyzed by western blotting.

(B) $Mdm2^{C462A}$ mutant protein binds p53, L5, and L11. $Mdm2^{+/+};p53^{ER/-}$ and $Mdm2^{m/m};p53^{ER/-}$ MEFs were treated with 100 nM 4-OHT for 24 hr. Cell extracts were immunoprecipitated with Mdm2 antibodies (2A10) and analyzed by western blotting with indicated antibodies. Loading control represents approximately 5% of cell lysate used for IP.

(C) The p53-binding activity of the $Mdm2^{C462A}$ mutant is similar to that of wild-type Mdm2. MEFs of indicated genotype were infected with retroviruses expressing a murine temperature-sensitive p53 (tsp53) mutant, $p53^{A135V}$. Cells were selected with puromycin and maintained at 39.5°C. Cell extracts were prepared after cells were cultured for 24 hr at 32°C and were immunoprecipitated with goat polyclonal anti-p53 antibody (FL-393, Santa Cruz) and analyzed by western blotting. Loading control represents approximately 5% of cell lysate used for IP.

from unchecked p53 activity. These data also suggest that the Mdm2-p53 interaction, in the absence of Mdm2-mediated p53 ubiquitination, cannot sufficiently suppress p53's transactivation activity, at least toward the *p21* gene.

To ascertain that the in vivo $Mdm2^{C462A}$ protein is able to interact physically with p53, whole-cell lysates, in the presence of 4-OHT, were isolated and analyzed for Mdm2's interaction with p53ER, and with ribosomal proteins L5 and L11 as controls, by immunoprecipitation-coupled western blotting (IP-western) (Figure 3B). The p53ER protein, as well as L5 and L11, was clearly coimmunoprecipitated along with the $Mdm2^{C462A}$ protein, and the levels of coimmunoprecipitated proteins correlated quantitatively with the levels of the proteins in the lysates. To determine the relative competence of the Mdm2-p53 interaction, we established cells stably expressing a temperature-sensitive p53 (tsp53) point mutant, $p53^{A135V}$ (Michalovitz et al., 1990), in $Mdm2^{C462A/C462A};p53^{-/-}$ MEFs, using a retroviral infection procedure. The tsp53 protein, carrying a substitution from alanine to valine at position 135, is inactive at 39°C, therefore allowing the MEFs to grow. The tsp53-expressing MEFs were cultured at 39°C to reach 80% confluence and then shifted to 32°C to resume wild-type p53 structure and activity. We chose two established cell lines expressing the same levels of tsp53 to facilitate comparison of its binding activity to Mdm2 and $Mdm2^{C462A}$. The p53-Mdm2 interaction was then analyzed by IP-western, using comparable protein levels of ectopic $p53^{A135V}$ and endogenous Mdm2 in the $Mdm2^{C462A/C462A};p53^{-/-}$ and the $Mdm2^{+/+};p53^{-/-}$ MEFs. As shown in Figure 3C, $p53^{A135V}$ was able to precipitate comparable amounts of wild-type and mutant $Mdm2^{C462A}$ protein. Thus, the mutant $Mdm2^{C462A}$ protein is fully capable of interacting physically with p53.

Mdm2 RING E3 Activity Is Required for p53 Degradation but Not Mdm2 Degradation under Physiological Conditions

Previous studies have shown that mutations in the Mdm2 RING finger domain lead to stabilization of not only p53 but also Mdm2 itself, indicating that the Mdm2 RING E3 ubiquitin ligase function is essential for promoting Mdm2 autodegradation. With the creation of $Mdm2^{C462A}$ knockin mice, we wished to revisit the role of the Mdm2 RING E3 ligase in regulating protein stability of p53 and Mdm2 itself under physiological conditions. We intercrossed $Mdm2^{+/C462A};p53^{-/-}$ mice to isolate three types of littermate *p53* null MEFs ($Mdm2^{+/+}$, $Mdm2^{+/C462A}$, and $Mdm2^{C462A/C462A}$). Under normal culturing conditions (DMEM + 10% FBS, 37°C, and 5% CO_2), all three types of MEFs grew rapidly and became immortal without undergoing replication crisis, consistent with their *p53* null status. We did not find obvious changes in the growth properties of the $Mdm2^{C462A/C462A};p53^{-/-}$ MEFs as compared to either $Mdm2^{+/+};p53^{-/-}$ or $Mdm2^{+/C462A};p53^{-/-}$ MEFs (data not shown). Blotting with anti-p53 antibody confirmed the *p53* null status of the MEFs (Figure 4A, p53 panel). To assess Mdm2 protein expression, we isolated whole-cell lysates from early-passage (passage 2) MEFs and determined the levels of Mdm2 by western blotting. Surprisingly, the levels of Mdm2 protein were essentially identical among the three *p53* null MEFs and were lower than that of wild-type MEFs (Figure 4A, Mdm2 panel). This is unexpected because, if the RING E3 is required for Mdm2 degradation, the mutant $Mdm2^{C462A}$ protein should accumulate in the $Mdm2^{C462A/C462A};p53^{-/-}$ MEFs, and the $Mdm2^{C462A}$ protein level should be higher in the $Mdm2^{C462A/C462A};p53^{-/-}$ MEFs than in the $Mdm2^{+/C462A};p53^{-/-}$ and $Mdm2^{+/+};p53^{-/-}$ MEFs. To directly compare protein stability between the wild-type Mdm2 and the $Mdm2^{C462A}$ mutant, we carried out a protein half-life assay using early-passage (passage 2) $Mdm2^{+/+};p53^{-/-}$ and $Mdm2^{C462A/C462A};p53^{-/-}$ MEFs. Consistently, the half-life was essentially identical between the wild-type and the RING mutant Mdm2; in both cases the half-life was about 20 min (Figure 4B), indicating that the Mdm2 RING E3 is not required for Mdm2 degradation, at least under *p53* null and low-Mdm2 conditions.

To assess potential effects of p53 on Mdm2 protein stability, p53 competence was restored in $Mdm2^{+/+};p53^{ER/-}$ and $Mdm2^{C462A/C462A};p53^{ER/-}$ MEFs by administration of 4-OHT to transactivate *Mdm2* gene expression and to achieve physiologically high levels of Mdm2 protein. Twenty-four hours after p53 function restoration, the half-life of Mdm2 was determined. In the presence of activated p53ER, both the wild-type Mdm2 and the $Mdm2^{C462A}$ mutant were degraded equally rapidly, and their half-lives of approximately 20 min (Figure 4C) were essentially identical to those measured in MEFs without p53 (Figure 4B), even though the $Mdm2^{C462A}$ protein was expressed to a very high level (as shown in Figure 3A). These data further suggest that high levels of $Mdm2^{C462A}$ in the 4-OHT-treated $Mdm2^{C462A/C462A};p53^{ER/-}$ MEFs are due to activation of p53ER but not stabilization of Mdm2. In contrast, the p53ER protein was rapidly degraded, with a half-life of 30 min, only in the $Mdm2^{+/+};p53^{ER/-}$ MEFs, but was essentially undegradable in the $Mdm2^{C462A/C462A};p53^{-/-}$ MEFs, which is consistent with the steady-state levels of p53ER in the two cells shown in Figure 3A. Thus, under physiological conditions, the Mdm2 RING E3 is required for p53 degradation, but not for Mdm2 degradation.

This conclusion is paradoxical to numerous in vitro studies showing that mutations in the Mdm2 RING finger result in stabilization of both p53 and Mdm2. To rule out the possibility that the process of generating the *Mdm2* RING mutant mice may have elicited an alternative Mdm2-destabilizing mechanism leading to $Mdm2^{C462A}$ mutant degradation, we ectopically expressed both the wild-type and the RING mutant Mdm2 in the $Mdm2^{C462A/C462A};p53^{-/-}$ MEFs and determined the half-life of the ectopic Mdm2. To distinguish ectopic Mdm2 from endogenous Mdm2, we used human HDM2 and the $Mdm2^{C462A}$ equivalent $HDM2^{C464A}$ mutant for the transfection and examined the ectopic protein by the HDM2-specific antibody 4B11. Notably, consistent with previous in vitro studies, only the wild-type, but not the

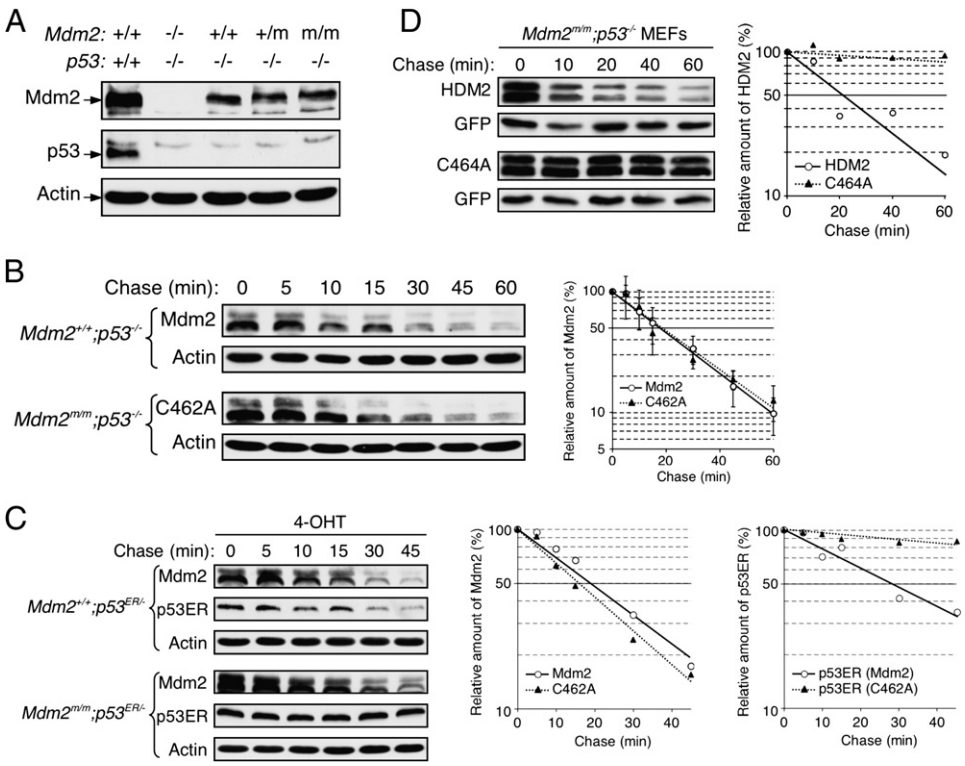

Figure 4. Mdm2 RING-Mediated E3 Ubiquitin Ligase Activity Is Dispensable for Mdm2 Degradation

(A) Mdm2 protein levels are similar in *Mdm2*$^{+/+}$;*p53*$^{-/-}$ and *Mdm2*$^{m/m}$;*p53*$^{-/-}$ MEFs. Total protein was isolated from passage 1 MEFs with indicated genotypes and analyzed by western blotting.

(B) Both Mdm2 and Mdm2^{C462A} proteins degrade similarly in *Mdm2*$^{+/+}$;*p53*$^{-/-}$ and *Mdm2*$^{m/m}$;*p53*$^{-/-}$ MEFs. Early-passage (P2) MEFs were treated with cycloheximide (50 μg/ml) and chased for the indicated times. The levels of Mdm2 were analyzed by western blotting. Actin served as a loading control. The amount of Mdm2 remaining at each time point was quantified by densitometry, normalized relative to the amount of Actin, and plotted to the right. The experiments were repeated with MEFs prepared from four different sets of embryos. Error bars represent the mean ± SD of four independent experiments.

(C) Both Mdm2 and Mdm2^{C462A} proteins degrade similarly in *Mdm2*$^{+/+}$;*p53*$^{ER/-}$ and *Mdm2*$^{m/m}$;*p53*$^{ER/-}$ MEFs. Early-passage (P2) MEFs of indicated genotype were treated with 100 nM of 4-OHT for 24 hr and analyzed identically as in (B). The amount of Mdm2 and p53ER remained at each time point was quantified by densitometry, normalized relative to the amount of Actin, and plotted to the right.

(D) Ectopically expressed HDM2^{C464A} RING mutant protein is resistant to degradation. *Mdm2*$^{m/m}$;*p53*$^{-/-}$ MEFs were transfected with plasmid DNA expressing HDM2 or HDM2^{C464A} along with a GFP plasmid. Twenty-four hours after transfection, the cells were treated with cycloheximide (50 μg/ml) and chased for the indicated times. Ectopically expressed HDM2 and HDM2^{C464A} were detected by HDM2-specific antibody 4B11. GFP was detected by anti-GFP antibody and served as transfection efficiency control. The amount of HDM2 remaining at each time point was quantified by densitometry, normalized relative to the amount of GFP, and plotted to the right.

RING mutant, HDM2 was rapidly degraded in the *Mdm2*$^{C462A/C462A}$;*p53*$^{-/-}$ MEFs. The half-life of the wild-type HDM2 was similar to that of endogenous Mdm2, at about 20 min, whereas the RING mutant HDM2 was resistant to degradation (Figure 4D). Thus, the data indicate that the Mdm2 RING E3 function is required for degradation of ectopically overexpressed Mdm2, but not for endogenously expressed Mdm2.

DNA Damage Induces Destabilization of Mdm2 Regardless of Mdm2 RING E3 Function

Previous studies have shown that Mdm2's half-life decreases after cells are treated with DNA-damaging agents (Stommel and Wahl, 2004). To determine whether the endogenous Mdm2^{C462A} mutant protein is also sensitive to DNA damage and subsequent rapid degradation, we treated early-passage *Mdm2*$^{+/+}$;*p53*$^{-/-}$ and *Mdm2*$^{C462A/C462A}$;*p53*$^{-/-}$ MEFs with 10 Gy gamma irradiation followed by a protein half-life assay. Consistent with a previous in vitro study, the half-life of wild-type Mdm2 was shortened after cells were exposed to gamma irradiation, from 20 min in untreated cells to approximately 5 min in treated cells (Figure 5A). Importantly, the half-life of the Mdm2^{C462A} mutant protein was also decreased from 20 min to about 5 min after gamma irradiation, an effect indistinguishable from that seen in the wild-type Mdm2 under DNA damage conditions. To assess DNA damage-induced destabilization of Mdm2 in the presence of p53, we first restored p53 function in *Mdm2*$^{+/+}$;*p53*$^{ER/-}$ and *Mdm2*$^{C462A/C462A}$;*p53*$^{ER/-}$ MEFs by administration of 4-OHT. We then treated the cells with 10 Gy gamma irradiation and determined the half-life of both Mdm2 and p53 (Figure 5B).

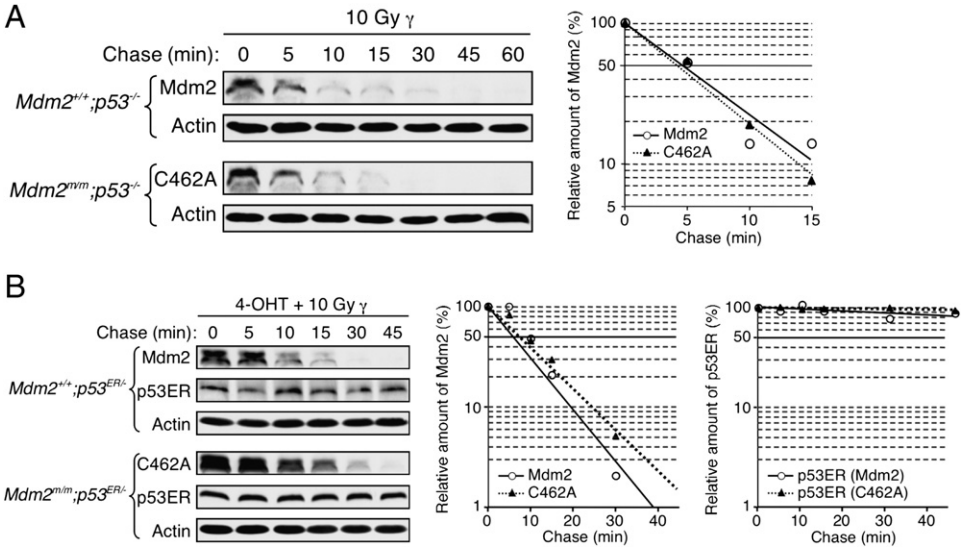

Figure 5. DNA Damage Induces Destabilization of Mdm2 Regardless of Mdm2 RING E3 Function

(A) Mdm2 and Mdm2^{C462A} were similarly destabilized in *Mdm2*$^{+/+}$;*p53*$^{-/-}$ and *Mdm2*$^{m/m}$;*p53*$^{-/-}$ MEFs after gamma irradiation. Early-passage (passage 2) MEFs of indicated genotypes were treated with 10 Gy of gamma irradiation. Three hours after treatment, the cells were analyzed for Mdm2 half-life as described above. The percentage of Mdm2 protein remaining at each time point was quantified by densitometry, normalized relative to the amount of Actin, and plotted to the right.

(B) Mdm2 and Mdm2^{C462A} were destabilized and p53ER was stabilized in *Mdm2*$^{+/+}$;*p53*$^{ER/-}$ and *Mdm2*$^{m/m}$;*p53*$^{ER/-}$ in a similar manner after gamma irradiation. Early-passage (passage 2) MEFs of indicated genotypes were assayed for Mdm2 and p53ER half-life in a way identical to that in (A).

Consistently, in spite of the presence of active p53ER, which induces expression of Mdm2, both the wild-type and RING mutant Mdm2 were rapidly degraded after gamma irradiation, with a half-life of less than 10 min for each protein. In contrast, the p53ER protein was stabilized after gamma irradiation, with a half-life greater than 45 min, in the presence of either wild-type or the RING mutant Mdm2. Thus, DNA damage induces destabilization of Mdm2, regardless of Mdm2's RING E3 ubiquitin ligase function.

Endogenous Mdm2^{C462A} Protein Is Polyubiquitinated and Degraded in a Proteasome-Dependent Manner

To determine whether ubiquitin-mediated proteolysis is involved in the degradation of the Mdm2^{C462A} mutant protein, we first examined the Mdm2 protein level after treating the *Mdm2*$^{+/+}$;*p53*$^{-/-}$ and *Mdm2*$^{C462A/C462A}$;*p53*$^{-/-}$ MEFs with MG132, which blocks the 26S proteasome-mediated proteolysis. Treating the cells with 25 μM of MG132 for 10 hr stabilized both the wild-type and the RING mutant Mdm2 to an equal extent (Figure 6A), indicating that ubiquitin-mediated proteolysis and the 26S proteasome are involved in the degradation of Mdm2, including the Mdm2^{C462A} mutant. To directly demonstrate Mdm2 ubiquitination, we transiently overexpressed p53 by adenovirus in the *Mdm2*$^{+/+}$;*p53*$^{-/-}$ and *Mdm2*$^{C462A/C462A}$;*p53*$^{-/-}$ MEFs to transactivate endogenous *Mdm2* and to achieve comparable high levels of wild-type and mutant Mdm2 protein. We then treated the cells with MG132 and lysed them directly in hot SDS lysis buffer (hot SDS buffer protects Ub-conjugated proteins from deubiquitination during sample preparation). To enrich the total amount of Mdm2 protein so that polyubiquitinated species could be detected, the cell lysates were immunoprecipitated with anti-Mdm2 antibody and resolved on an SDS-PAGE gel followed by western blotting, using anti-Mdm2 antibody. We estimate that approximately 1.5 × 10^7 cells (from three p100 plates) were used for each IP sample. As shown in Figure 6B, high-molecular-weight ladders/smears, indicative of polyubiquitinated species, were observed in both the wild-type and the RING mutant Mdm2, and the smears were more pronounced after MG132 treatment (Figure 6B, Long exp), indicating that these smears are polyubiquitinated Mdm2. Importantly, the high-molecular-weight ladders/smears were observed at equal levels for Mdm2 isolated from lysates of both *Mdm2*$^{+/+}$;*p53*$^{-/-}$ and *Mdm2*$^{C462A/C462A}$;*p53*$^{-/-}$ MEFs. We believe that the high-molecular-weight ladders/smears observed in the Mdm2^{C462A} mutant are polyubiquitinated Mdm2^{C462A} protein, because they were identical to those from the wild-type Mdm2 and were enhanced by MG132 treatment. Thus, the RING mutant Mdm2^{C462A} can be polyubiquitinated in vivo. Finally, to confirm that the in vivo Mdm2^{C462A} mutant is indeed inactive in promoting p53 polyubiquitination, we transiently expressed p53 in three *p53* null MEFs (*Mdm2*$^{-/-}$;*p53*$^{-/-}$, *Mdm2*$^{+/+}$;*p53*$^{-/-}$, and *Mdm2*$^{C462A/C462A}$;*p53*$^{-/-}$) and examined p53 polyubiquitination by a hot SDS-coupled straight western blotting assay. As shown in Figure 6C, a high-molecular-weight ladder of p53—indicative of polyubiquitinated p53 species—was observed only in

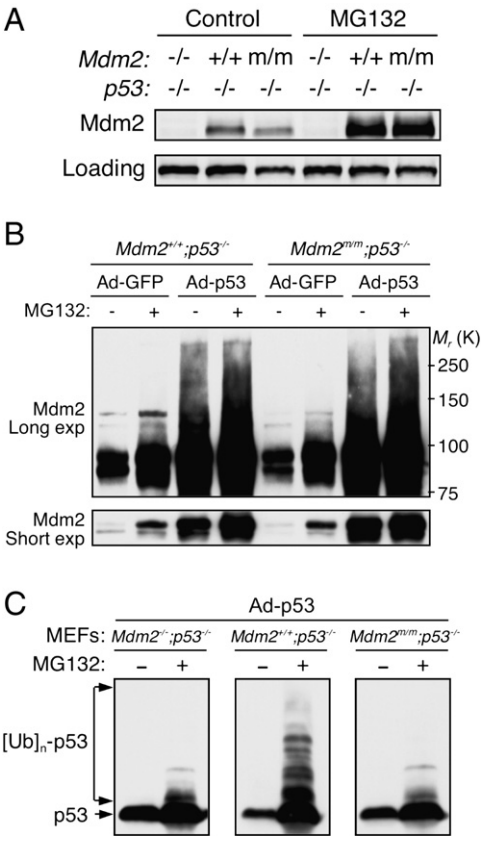

Figure 6. Mdm2^{C462A} Mutant Protein Is Degraded through Proteasome-Dependent Proteolysis

(A) Mdm2 and Mdm2^{C462A} can be equally stabilized in MEFs by MG132. Early-passage (passage 2) MEFs of *Mdm2*$^{-/-}$;*p53*$^{-/-}$, *Mdm2*$^{+/+}$;*p53*$^{-/-}$, and *Mdm2*$^{m/m}$;*p53*$^{-/-}$ genotypes were either untreated or treated with 25 μM of MG132 for 10 hr. Cell lysates were analyzed for Mdm2 by western blotting. A nonspecific band detected by the Mdm2 antibody (2A10) served as a loading control.

(B) Both Mdm2 and Mdm2^{C462A} can be polyubiquitinated in MEFs. Early-passage (passage 2) MEFs of *Mdm2*$^{+/+}$;*p53*$^{-/-}$ and *Mdm2*$^{m/m}$;*p53*$^{-/-}$ genotypes were infected with adenoviruses expressing either GFP or human p53. Two days after infection, the cells were treated with 20 μM of MG132 for 8 hr and cell lysates were harvested. Mdm2 protein was immunoprecipitated with anti-Mdm2 antibody (2A10) and analyzed by western blotting with 2A10. Both long and short exposures are shown.

(C) Endogenous Mdm2^{C462A} protein cannot promote p53 polyubiquitination. MEFs of *Mdm2*$^{-/-}$;*p53*$^{-/-}$, *Mdm2*$^{+/+}$;*p53*$^{-/-}$, and *Mdm2*$^{m/m}$;*p53*$^{-/-}$ genotypes were infected with adenovirus expressing human p53 and treated with 20 μM of MG132 as in (B). Cell lysates were analyzed by western blotting using antibodies to p53 (DO-1).

Mdm2$^{+/+}$;*p53*$^{-/-}$ MEFs, but not in *Mdm2*$^{-/-}$;*p53*$^{-/-}$ and *Mdm2*$^{C462A/C462A}$;*p53*$^{-/-}$MEFs, indicating that the Mdm2^{C462A} mutant is unable to promote p53 polyubiquitination.

DISCUSSION

Mdm2 is frequently amplified/overexpressed in human tumors, many of which lack mutations in the *p53* gene (Leach et al., 1993), leading to the assumption that Mdm2 overexpression is functionally equivalent to p53 mutation (Momand et al., 1998). Our initial rationale for generating *Mdm2* RING mutant mice was to test whether a high level of Mdm2, due to lack of self-ubiquitination and degradation, might directly bind to and inhibit the activity of p53, causing cancer formation in the absence of p53 mutations; such a model would recapitulate human cancers with Mdm2 amplification. However, knockin of the *Mdm2* RING finger mutation in the mouse resulted instead in embryonic lethality and revealed two unexpected insights into the Mdm2-imposed p53 repression: (1) the Mdm2-p53 physical interaction, in the absence of Mdm2-mediated p53 ubiquitination, cannot suppress p53 activity sufficiently to allow mouse early embryonic development; and (2) the Mdm2 RING-mediated E3 ubiquitin ligase function is not required for Mdm2 degradation.

Our data raise questions about a widely held view of the mechanism of Mdm2-mediated p53 inhibition, in which it is believed that the binding of Mdm2 with p53's N-terminal transactivation domain interferes with p53's interaction with basal transcriptional machinery, blocking p53's transcriptional activity (Oliner et al., 1993; Thut et al., 1997). Although we cannot rule out the possibility that the physical interaction between Mdm2 and p53 still inhibits p53 function to a certain extent, or toward a specific set of target genes, our study has otherwise indicated that Mdm2 binding alone, without inducing p53 ubiquitination, is unable to suppress p53 activity in vivo, at least to a degree allowing mouse embryos to develop. Even when expressed at a very high level in the *Mdm2*$^{C462A/C462A}$;*p53*$^{ER/-}$ MEFs upon 4-OHT induction, the mutant Mdm2^{C462A}, unlike wild-type Mdm2, cannot suppress p53 activity, at least toward *p21* and *Mdm2* induction (Figure 3A). This finding suggests that Mdm2 RING E3 activity is likely the major—if not the only—biochemical activity required to suppress p53, regardless of whether by direct ubiquitination of p53 or by ubiquitination of intermediary proteins (Minsky and Oren, 2004). The Mdm2-mediated p53 ubiquitination could serve multiple distinct functions, such as tagging p53 for proteasomal degradation, promoting p53 cytoplasmic translocation, and directly suppressing p53 transcriptional activity by, for example, blocking access of transcription cofactors. In this regard, it is tempting to say that the principal mechanism involved in activating p53 upon a variety of cellular stresses could be simply to inhibit Mdm2's E3 ubiquitin ligase activity, thereby releasing p53 from ubiquitination-mediated repression. The notion that blocking Mdm2-induced p53 ubiquitination, without disrupting the Mdm2-p53 interaction, could be sufficient to release p53 activity provides a potential unified mechanism for the action of many Mdm2 inhibitors, such as ARF and L11, whose association with Mdm2 and inhibition of the Mdm2 E3 ubiquitin ligase function would be sufficient to activate p53 without necessarily disrupting the Mdm2-p53 physical interaction.

Our data also call into question the role of Mdm2's RING-mediated E3 ubiquitin ligase function in Mdm2 self-degradation. Previous studies using in vitro ectopic

expression systems have shown that mutations in the Mdm2 C-terminal RING domain result in stabilization of both p53 and Mdm2, indicating that the RING E3 is important for Mdm2 autoubiquitination and -degradation. Using an in vivo system, which skirts the complication of protein overexpression, we demonstrate that the Mdm2 RING E3 is not essential for Mdm2 degradation. The findings that, under both unstressed and genotoxically stressed conditions, the $Mdm2^{C462A}$ mutant protein has a short half-life indistinguishable from that seen in wild-type Mdm2 (Figures 4 and 5), and that the $Mdm2^{C462A}$ mutant protein is sensitive to MG132-induced stabilization (Figure 6), predict the existence of other ubiquitin E3s for Mdm2 degradation. Consistent with this notion, a recent study has shown that the histone acetyltransferase PCAF can negatively regulate Mdm2 by promoting Mdm2 ubiquitination and degradation (Linares et al., 2007). We do not rule out that Mdm2 autoubiquitination may occur when the protein is expressed at extremely high levels, or that the C462A point mutation itself may cause unforeseen effects on protein stability. However, given the stark deviation between the in vitro and in vivo results for Mdm2 autodegradation revealed by the $Mdm2^{C462A}$ mutant knockin, alternative mechanisms for Mdm2 ubiquitination and degradation, including PCAF-induced degradation, warrant further investigation with an in vivo system.

The finding that inhibiting Mdm2-induced p53 ubiquitination, while retaining Mdm2-p53 binding, results in embryonic lethality has intriguing implications. It has been demonstrated that Mdm2 and Mdm4 (a.k.a. Mdmx) interact with each other via their respective RING domains, and that the Mdm2 RING finger mutation disrupts Mdm2-Mdm4 binding (Kawai et al., 2003). We have not determined whether, under physiological conditions, the $Mdm2^{C462A}$ mutant protein can interact with Mdm4. Whether the Mdm2-Mdm4 interaction is essential for activating Mdm2's E3 ubiquitin ligase activity toward p53, and whether Mdm2-mediated p53 ubiquitination plays any role in determining p53's decision between growth arrest and apoptosis, remain interesting questions that can now be addressed with the *Mdm2* RING mutant mouse model.

EXPERIMENTAL PROCEDURES

Generation of $Mdm2^{C462A}$ Mutant Mice

Murine 129/Sv genomic DNA containing the last six exons (7–12) of *Mdm2* was a gift from Dr. Lozano (University of Texas, M.D. Anderson Cancer Center). The targeting vector was constructed in a *PGK* neo vector. A cysteine to alanine substitution was introduced in codon 462 using site-directed mutagenesis, and a new Eag1 restriction site was generated at the same time. The final construct was sequenced using overlapping primers. Electroporation of 129/Sv-derived AB2.2 ES cells was performed by the UNC Animal Models Core Facility. DNA isolated from 192 G418-resistant ES colonies was subjected to BamH1 digestion followed by Southern blotting analysis using a probe covering intron 9 between exons 9 and 10. Positive clones were further confirmed for the presence of the C462A substitution by PCR amplification of genomic DNA using primers flanking exon 12, followed by Eag1 digestion. Two positive clones were injected into C57BL/6 blastocysts, and the blastocysts were transferred into pseudopregnant CD1 female recipients. The resulting chimeric males were mated with C57BL/6 females. Germline transmissions were confirmed by Southern blotting and PCR analysis.

Mouse Breeding, Maintenance, and Genotyping

Eleven chimeric mice generated from ES cells were mated with C57BL/6 females. The progeny agouti mice were genotyped by PCR and *Eag1* digestion to screen for germline transmission. The germline-transmitted $Mdm2^{+/C462A}$ heterozygous mice were crossed with *Ella-Cre* transgenic mice (The Jackson Laboratory) to delete the *neomycin* selection marker and were backcrossed to C57BL/6 mice for four generations and maintained on a mixed 129/Sv × C57BL/6 background. The mice and embryos were analyzed in comparison to their own littermates. The *p53* null mice ($p53^{-/-}$) were purchased from The Jackson Laboratory. $p53ER^{TAM}$ knockin mice and genotyping of the $p53ER^{TAM}$ alleles were described previously (Christophorou et al., 2005). Mice were bred and maintained strictly under protocols (#07-056.0-A) approved by the Institutional Animal Care and Use Committee in the UNC Animal Care Facility. The $Mdm2^{C462A}$ mutant allele was identified by Eag1 digestion of PCR product using primers 5′-GCTTCTTGGTTGAAGGGTTGAATTGATGC-3′ and 5′-GTTCTTCTGTAGCCCTTGATGAGGAAG-3′; or 5′-GCAGCCAAGAAAGCGTGAAAGAGTTG-3′ and 5′-ACAGAGCAGGTCAGCTAGTTGAAG-3′ for *Mdm2*. The $Mdm2^{C462A}$ mutation was further confirmed by DNA sequencing of PCR-amplified tail DNA. PCR primers for wild-type (p53-X7, 5′-GGATGGTGGTATACTCAGAGCC-3′; p53-X6, 5′-ACAGCGTGGTGGTACCTTAT-3′) and mutant (p53-X7; NEO18.5, 5′-TCCTCGTGCTTTACGGTATC-3′) *p53* alleles were described by The Jackson Laboratory.

Southern Blotting and RT-PCR Analysis

Southern blotting analysis was performed using NEN Life Science GeneScreen kit with a 1 Kb probe that recognizes intron 9 of *Mdm2* as indicated in Figure 1A. For RT-PCR, total RNA was extracted using the Total RNA Isolation kit (Promega). The primers were as follows: *Mdm2*, 5′-CTAGTTGAAGTAAGTTAGCAC-3′ and 5′-AGGAGAGTGACGACTATTC-3′; *p53*, 5′-TACCATCATCACACTGGAAGAC-3′ and 5′-TTTATGGCGGGAAGTAGAC-3′; *β-actin*, 5′-CACGGCATTGTAACCAACTG-3′ and 5′-CTGGGTCATCTTTTCACGGT-3′.

Histological and Histochemical Analysis of Mouse Embryos

Embryos were fixed overnight in 10% formalin (buffered to neutral). The formalin-fixed embryos were paraffin embedded at the Histopathology Core Facility. Sections (5 μm) were cut and stained with hematoxylin and eosin (H&E).

Cell Culture

Primary MEF cells were cultured in a 37°C incubator with 5% CO_2 in DMEM supplied with 10% FBS and penicillin (100 IU/ml)/streptomycin (100 μg/ml). Cells were maintained by 3T3 protocol, and cell number was counted with a hematocytometer. pBabe retrovirus vector encoding murine *p53* was a gift from Dr. Peiqing Sun (Scripps, CA), and the temperature-sensitive *p53* (*tsp53*) mutant $p53^{A135V}$ was made by PCR-based site-directed mutagenesis. *p53* null MEFs expressing $Mdm2^{+/+}$ and $Mdm2^{C462A/C462A}$ were infected with retroviruses carrying *tsp53* at 37°C, selected with puromycin (2.5 μg/ml) for 3 days at 39.0°C, and maintained at 39.0°C until shifting temperature to 32°C for p53 activation. Procedures for production and infection of retroviruses and adenoviruses were described previously (Itahana et al., 2003). For activation of $p53ER^{TAM}$, 100 nM 4-hydroxytamoxifen (Sigma) dissolved in 100% ethanol was added to the culture medium.

Protein Analysis

Mouse monoclonal Mdm2 (2A-10 and 4B11, Calbiochem), p53 (NCL-505, Novocastra; DO-1,Lab Vision/Neomarkers), actin (MAB1501, Chemicon International), goat polyclonal p53 (FL-393; Santa Cruz), and rabbit polyclonal p53 (CM5, Novocastra) antibodies were purchased commercially. Rabbit polyclonal antibodies to p21 were gifts from Dr. Yue Xiong (UNC-Chapel Hill). Rabbit polyclonal antibodies to L5 and L11 were previously described (Lindstrom et al., 2007). Cells

were lysed in 0.1% NP-40 buffer for immunoprecipitation and 0.5% NP-40 buffer for straight western blotting. Procedures and conditions for immunoprecipitation and immunoblotting were described previously (Itahana et al., 2003). The half-life of Mdm2 protein was measured by treating cells with cycloheximide (50 μg/ml) for indicated length of time. The Mdm2 level was analyzed by western blotting, and the intensity of the bands in the linear range of exposure was quantified by densitometry.

In Vivo Ubiquitination Assay

MEF cells were lysed in 1% SDS lysis buffer (1% SDS and 1% NP-40 in PBS). The cell lysates were diluted ten times with 0.1% NP-40-PBS containing 1 mM phenylmethylsulfonyl fluoride (PMSF). The diluted lysates were precleared with Sepharose CL4B beads (Sigma) for 30 min and then immunoprecipitated with anti-Mdm2 antibody (2A10) overnight at 4°C, followed by incubation with protein A beads (Pierce) for 2 hr at 4°C. The beads were washed four times with cold 0.1% NP-40-PBS containing 1 mM PMSF. The beads were then incubated in 1× SDS loading buffer.

ACKNOWLEDGMENTS

We thank Chad Deisenroth, Yue Xiong, Norman Sharpless, Guillermina Lozano, Feng Bai, and Xinhai Pei for their helpful advice and technical assistance; and Peiqing Sun for providing invaluable reagents. H.V.C. is a recipient of a Fellowship from the Lineberger Cancer Center's Cancer Cell Biology predoctoral Training Program. Y.Z. is a recipient of a Career Award in Biomedical Science from the Burroughs Wellcome Fund and a Howard Temin Award from the National Cancer Institute. This study was supported by grants from the NIH and the Leukemia Research Foundation.

Received: January 22, 2007
Revised: June 22, 2007
Accepted: September 4, 2007
Published: October 15, 2007

REFERENCES

Christophorou, M.A., Martin-Zanca, D., Soucek, L., Lawlor, E.R., Brown-Swigart, L., Verschuren, E.W., and Evan, G.I. (2005). Temporal dissection of p53 function in vitro and in vivo. Nat. Genet. *37*, 718–726.

Elenbaas, B., Dobbelstein, M., Roth, J., Shenk, T., and Levine, A.J. (1996). The MDM2 oncoprotein binds specifically to RNA through its RING finger domain. Mol. Med. *2*, 439–451.

Francoz, S., Froment, P., Bogaerts, S., De Clercq, S., Maetens, M., Doumont, G., Bellefroid, E., and Marine, J.C. (2006). Mdm4 and Mdm2 cooperate to inhibit p53 activity in proliferating and quiescent cells in vivo. Proc. Natl. Acad. Sci. USA *103*, 3232–3237.

Geyer, R.K., Yu, Z.K., and Maki, C.G. (2000). The MDM2 RING-finger domain is required to promote p53 nuclear export. Nat. Cell Biol. *2*, 569–573.

Grossman, S.R., Perez, M., Kung, A.L., Joseph, M., Mansur, C., Xiao, Z.X., Kumar, S., Howley, P.M., and Linvingston, D.M. (1998). p300/MDM2 complexes participate in MDM2-mediated p53 degradation. Mol. Cell *2*, 405–415.

Haupt, Y., Maya, R., Kazaz, A., and Oren, M. (1997). Mdm2 promotes the rapid degradation of p53. Nature *387*, 296–299.

Honda, R., Tanaka, H., and Yasuda, H. (1997). Oncoprotein MDM2 is a ubiquitin ligase E3 for tumor suppressor p53. FEBS Lett. *420*, 25–27.

Honda, R., and Yasuda, H. (2000). Activity of MDM2, a ubiquitin ligase, toward or itself is dependent on the RING finger domain of the ligase. Oncogene *19*, 1473–1476.

Itahana, K., Bhat, K.P., Jin, A., Itahana, Y., Hawke, D., Kobayashi, R., and Zhang, Y. (2003). Tumor suppressor ARF degrades B23, a nucleolar protein involved in ribosome biogenesis and cell proliferation. Mol. Cell *12*, 1151–1164.

Jackson, M.W., and Berberich, S.J. (2000). MdmX protects p53 from Mdm2-mediated degradation. Mol. Cell. Biol. *20*, 1001–1007.

Jones, S.N., Roe, A.E., Donehower, L.A., and Bradley, A. (1995). Rescue of embryonic lethality in Mdm2-deficient mice by absence of p53. Nature *378*, 206–208.

Kawai, H., Wiederschain, D., and Yuan, Z.M. (2003). Critical contribution of the MDM2 acidic domain to p53 ubiquitination. Mol. Cell. Biol. *23*, 4939–4947.

Ko, L.J., and Prives, C. (1996). p53: Puzzle and paradigm. Genes Dev. *10*, 1054–1072.

Kostic, M., Matt, T., Martinez-Yamout, M.A., Dyson, H.J., and Wright, P.E. (2006). Solution structure of the Hdm2 C2H2C4 RING, a domain critical for ubiquitination of p53. J. Mol. Biol. *363*, 433–450.

Kubbutat, M.H.G., Jones, S.N., and Vousden, K.H. (1997). Regulation of p53 stability by Mdm2. Nature *387*, 299–303.

Leach, F.S., Tokino, T., Meltzer, P., Burrell, M., Oliner, J.D., Smith, S., Hill, D.E., Sidransky, D., Kinzler, K.W., and Vogelstein, B. (1993). p53 Mutation and MDM2 amplification in human soft tissue sarcomas. Cancer Res. *53*, 2231–2234.

Lin, J., Chen, J., and Levine, A.J. (1994). Several hydrophobic amino acids in the p53 amino-terminal domain are required for transcriptional activation, binding to MDM-2 and the adenovirus 5 E1B 55-kD protein. Genes Dev. *8*, 1235–1246.

Linares, L.K., Kiernan, R., Triboulet, R., Chable-Bessia, C., Latreille, D., Cuvier, O., Lacroix, M., Le Cam, L., Coux, O., and Benkirane, M. (2007). Intrinsic ubiquitination activity of PCAF controls the stability of the oncoprotein Hdm2. Nat. Cell Biol. *9*, 331–338.

Lindstrom, M.S., Jin, A., Deisenroth, C., White Wolf, G., and Zhang, Y. (2007). Cancer-associated mutations in the MDM2 zinc finger domain disrupt ribosomal protein interaction and attenuate MDM2-induced p53 degradation. Mol. Cell. Biol. *27*, 1056–1068.

Lohrum, M.A.E., Ashcroft, M., Kubbutat, M.H.G., and Vousden, K.H. (2000). Identification of a cryptic nucleolar-localization signal in MDM2. Nat. Cell Biol. *2*, 179–181.

Luna, R.M., Wagner, D.S., and Lozano, G. (1995). Rescue of early embryonic lethality in mdm2-deficient mice by deletion of p53. Nature *378*, 203–206.

Michalovitz, D., Halevy, O., and Oren, M. (1990). Conditional inhibition of transformation and of cell proliferation by a temperature-sensitive mutant of p53. Cell *62*, 671–680.

Minsky, N., and Oren, M. (2004). The RING domain of Mdm2 mediates histone ubiquitylation and transcriptional repression. Mol. Cell *16*, 631–639.

Momand, J., Zambetti, G.P., Olson, D.C., George, D., and Levine, A.J. (1992). The mdm-2 oncogene product forms a complex with the p53 protein and inhibits p53-mediated transactivation. Cell *69*, 1237–1245.

Momand, J., Jung, D., Wilczynski, S., and Niland, J. (1998). The MDM2 gene amplification database. Nucleic Acids Res. *26*, 3453–3459.

Oliner, J.D., Pietenpol, J.A., Thiagalingam, S., Gyuris, J., Kinzler, K.W., and Vogelstein, B. (1993). Oncoprotein MDM2 conceals the activation domain of tumor suppressor p53. Nature *362*, 857–860.

Poyurovsky, M.V., Jacq, X., Ma, C., Karni-Schmidt, O., Parker, P.J., Chalfie, M., Manley, J.L., and Prives, C. (2003). Nucleotide binding by the Mdm2 RING domain facilitates Arf-independent Mdm2 nucleolar localization. Mol. Cell *12*, 875–887.

Poyurovsky, M.V., Priest, C., Kentsis, A., Borden, K.L., Pan, Z.Q., Pavletich, N., and Prives, C. (2007). The Mdm2 RING domain C-terminus is required for supramolecular assembly and ubiquitin ligase activity. Embo J. *26*, 90–101. Published online December 14. 10.1038/sj.emboj.7601465.

Ringshausen, I., O'Shea, C.C., Finch, A.J., Swigart, L.B., and Evan, G.I. (2006). Mdm2 is critically and continuously required to suppress lethal p53 activity in vivo. Cancer Cell *10*, 501–514.

Sharp, D.A., Kratowicz, S.A., Sank, M.J., and George, D.L. (1999). Stabilization of the MDM2 oncoprotein by interaction with the structurally related MDMX protein. J. Biol. Chem. *274*, 38189–38196.

Stad, R., Ramos, Y.F.M., Litle, N., Grivell, S., Attema, J., van der Eb, A.J., and Jochmsen, A.G. (2000). Hdmx stabilizes Mdm2 and p53. J. Biol. Chem. *275*, 28039–28044.

Stommel, J.M., and Wahl, G.M. (2004). Accelerated MDM2 auto-degradation induced by DNA-damage kinases is required for p53 activation. EMBO J. *23*, 1547–1556.

Tanimura, S., Ohtsuka, S., Mitsui, K., Shirouzu, K., Yoshimura, A., and Ohtsubo, M. (1999). MDM2 interacts with MDMX through their RING finger domains. FEBS Lett. *447*, 5–9.

Thut, C.J., Goodrich, J.A., and Tjian, R. (1997). Repression of p53-mediated transcription by MDM2, a dual mechanism. Genes Dev. *11*, 1974–1986.

Toledo, F., Krummel, K.A., Lee, C.J., Liu, C.W., Rodewald, L.W., Tang, M., and Wahl, G.M. (2006). A mouse p53 mutant lacking the proline-rich domain rescues Mdm4 deficiency and provides insight into the Mdm2-Mdm4-p53 regulatory network. Cancer Cell *9*, 273–285.

Yang, Y., Li, C.C., and Weissman, A.M. (2004). Regulating the p53 system through ubiquitination. Oncogene *23*, 2096–2106.